Macrophage-Like Blood Cells Are Involved in Inter-Tissue Communication to Activate JAK/STAT Signaling That Induces Antitumor Turandot Proteins in Drosophila Fat Body via the TNF-JNK Pathway

Juri Kinoshita , Yuriko Kinoshita , Tadashi Nomura , and Yoshihiro H. Inoue *

Posted Date: 10 October 2024

doi: 10.20944/preprints202410.0708.v1

Keywords: Drosophila; Hematopoietic cell tumor; Innate immune system; Cytokines; JNK pathway; TNF family; JAK-STAT pathway

Article

Macrophage-like Blood Cells are Involved in Inter-Tissue Communication to Activate JAK/STAT Signaling that Induces Antitumor Turandot Proteins in Drosophila Fat Body via the TNF-JNK Pathway

Juri Kinoshita [1,2], Yuriko Kinoshita [1], Tadashi Nomura [1,2] and Yoshihiro H. Inoue [1,*]

[1] Biomedical Research Center, Kyoto Institute of Technology, Matsugasaki, Sakyo, Kyoto, 606-0962, Japan
[2] Graduate School of Science and Technology, Kyoto Institute of Technology, Matsugasaki, Sakyo, Kyoto, 606-8585, Japan
* Correspondence: yhinoue@kit.ac.jp; Tel.: +81-75-(724)7876

Abstract: Turandot (Tot) family proteins, which are induced via the JAK/STAT pathway after infection, also suppress lymph gland tumors in *Drosophila mxc*^{mbn1} mutant larvae. We investigated the potential role of hemocytes in *Tot* induction in tumor-bearing mutants by immunostaining and RNAi experiments. Normal hemocytes transplanted into mutant larvae were recruited to the tumor and fat body (FB), suggesting that these cells transmit tumor-related information. The transplanted hemocytes ectopically expressed Unpaired3 (Upd3), which is necessary to activate JAK/STAT. Eiger, a *Drosophila* Tumor necrosis factor (TNF) ortholog, was highly expressed in tumors. Depletion of the Eiger receptor in hemocytes reduced *Tot* levels and eventually enhanced tumor growth. The c-Jun N-terminal kinase (JNK) pathway, acting downstream of the receptor, was also activated in the hemocytes of mutants. Downregulation of the JNK pathway in hemocytes inhibited *Tot* induction, leading to enhanced tumor growth. These results suggest that the *upd3* expression in hemocytes depends on the Eiger-JNK pathway. We propose that after Eiger activates the JNK pathway in hemocytes on the tumor, cells expressing Upd3 are recruited to the FB. Upd3 then activates JAK/STAT to induce the expression of antitumor proteins. This study highlights the intricate communication between tissues via blood cells during tumor suppression.

Keywords: Drosophila; hematopoietic cell tumor; Innate IMMUNE system; Cytokines; JNK pathway; TNF family; JAK-STAT pathway

1. Introduction

Innate immunity is the first line of defense against infectious pathogens and tumor cells. Although insects, including *Drosophila*, do not have an acquired immune system, they exhibit immunological responses against microbes, parasite eggs, wounds, and tumors [1]. When microbial pathogens enter the body, humoral factors are induced. The fat body (FB) produces secreted proteins of low molecular weight, such as antimicrobial peptides (AMPs) and Turandot proteins (Tots) [2–4]. Depending on the type of invader (fungi, gram-negative bacteria, or gram-positive bacteria), different proteins are produced in the FB. Each AMP is induced by one or both Toll- and Imd-mediated signaling pathways [4], homologous to the mammalian Toll-like receptor (TLR) and Tumor necrosis factor (TNF) pathways, respectively [5,6]. Five major AMPs (Drosomycin, Defensin, Diptericin, Metchnikowin, and AttacinA) are induced in the tumor-bearing mutant larvae and have cytotoxic effects against tumors [7–9].

In addition to these well-known innate immunity pathways, the JAK/STAT signaling pathway plays a critical role in inducing another immune-responsible protein family called the Tot after infection [10]. When Unpaired (Upd) cytokines, such as Upd3, bind to their receptor, Domeless (Dome), the JAK/STAT pathway is activated in the cytoplasm [11]. Consequently, the transcription of *Tot* family genes is induced in FB [6,12]. Similar to AMPs, TotB and TotF proteins induced by the JAK/STAT pathway also have cytotoxic effects against tumors. These Tot proteins are induced in FB

 doi:10.20944/preprints202410.0708.v1

and incorporated into circulating hemocytes [13]. As a result, apoptosis is observed in the lymph gland (LG) tumors in the induction of AMPs and Tots, and tumor cell proliferation is also inhibited in Tots. However, the mechanism by which the effect of Tots on LG tumors located away from the FB has not yet been characterized.

The c-Jun N-terminal kinase (JNK) pathway is also activated in response to diverse intracellular stresses including tumors [14]. When a cytokine called Eiger, corresponding to a mammalian TNF family protein, binds to its receptors composed of Wengen and Grindelwald, they activate the JNK signaling pathway in the cytoplasm, including Hep, corresponding to JNKK, and Bsk, corresponding to JNK [15]. Activated Bsk phosphorylates and activates the transcription factor Jra, which induces the transcription of *upd* genes encoding ligands for the JAK/STAT pathway [16]. However, the interaction between these signaling pathways in mxc^{mbn1} larvae remains to be elucidated.

Hemocytes in the hemolymph, which are classified as plasmatocytes, lamellocytes, and crystal cells also play critical roles in eliminating pathogens [17]. Plasmatocytes, the equivalent of mammalian macrophages, comprise 95% of all *Drosophila* hemocytes and play essential roles in the cellular immune response such as phagocytosis [18,19]. During the larval stage, new hemocytes are produced in a hematopoietic tissue called the LG [20]. In larvae hemizygous for a loss-of-function mutation in the *multi sex combs* (*mxc*) gene, the hemocyte precursor cells in the LG overproliferate and differentiate abnormally [7,21–23]. The hemocyte precursor cells in the LG of mxc^{mbn1} mutant larvae become malignant and invade other tissues [21,24]. When mutant LG cells are transplanted into the abdominal cavity of normal flies, they continue to proliferate and infiltrate other adult tissues. Some aberrant hemocytes expressing undifferentiated markers are released into the hemolymph. These leukemia-like phenotypes are lethal to mutant larvae from the third-instar larval to the pupal stages [7,23,24]. In response to LG tumors, three innate immune pathways, the Toll-mediated, Imd-mediated, and JAK/STAT pathways, are activated to induce five major AMPs and four Tots in the FB of mxc^{mbn1} larvae [7,13]. Consequently, these AMPs stimulate apoptosis specifically in LG tumors [7–9]. For AMPs to be induced in FB, distant from the LG tumor, the information relevant to the presence of tumor cells must be transmitted to FB. Mutant hemocytes, as well as normal hemocytes transplanted from control larvae, are preferentially associated with LG tumors in mutant larvae [9]. However, whether hemocytes are recruited to FB efficiently in mxc^{mbn1} has not been investigated. The possibility that the recruitment of hemocytes to this tissue is due to the tumor characteristics of the mutant hemocytes has not been ruled out. To clarify, we investigated whether hemocytes transplanted from normal larvae were recruited more efficiently to mutant FB than to control tissue.

The depletion of TotB and TotF compromises apoptosis and enhances tumor cell proliferation [13]. However, the mechanism by which the JAK/STAT pathway is activated in FB has not been studied. Therefore, we aimed to clarify whether circulating hemocytes play a critical role in conveying tumor information to FB to activate the JAK/STAT pathway. Upd3, a ligand of the JAK/STAT pathway, produced by tumor cells signal the endocrine tissue to activate the JAK/STAT pathway [11]. Our previous study also showed that hemocytes from mxc^{mbn1} larvae ectopically express Upd3; consequently, this pathway is activated [13]. Thus, we also aimed to elucidate the mechanism by which the JAK/STAT signaling pathway is activated in FB via circulating hemocytes in response to LG tumors.

In the present study, we first examined whether *upd3* expression was required to induce Tot mRNA expression in FB, that is, the activation of the JAK/STAT pathway. We further investigated the effects of ectopic expression on LG tumor growth. Second, we focused on the mechanism by which Upd3 was highly expressed in the hemocytes of mxc^{mbn1} larvae. The TNF-like cytokine Eiger is expressed in the tumors of *Drosophila* imaginal discs and activates the JNK pathway [25]. Therefore, we investigated whether Eiger was highly expressed in the LG tumors of mxc^{mbn1} larvae. Third, we examined whether Eiger expression in LG tumors was required to activate the JNK pathway in circulating hemocytes. We then assessed whether the JNK pathway down-stream of the Eiger receptors in circulating hemocytes was required to activate the JAK/STAT pathway in FB. Additionally, we examined their effects on the growth of LG tumors. Based on these results, we proposed a model to explain how the higher expression of Eiger in LG tumors of mxc^{mbn1} larvae leads

 doi:10.20944/preprints202410.0708.v1

to the activation of the JAK/STAT pathway and, ultimately, induction of *Tot* expression in FB. AMPs and Tots secreted from FB are taken up by plasmatocytes of mutant larvae [7,13]. Thus, we also determined whether Tot proteins were taken up by macrophage-like plasmatocytes and transported to the tumor. The current results will be important for the future analysis of this tumor suppression mechanism, which may involve inter-tissue communication via hematopoietic cells, in *Drosophila* and other animal models.

2. Results

2.1. Increase in Normal Hemocytes Associated with the FB in mxc^{mbn1} Mutant Larvae Harboring the LG Tumor

Normal circulating hemocytes are recruited to the LG tumor more efficiently in mutant larvae than in normal larvae when the cells are transplanted into mutant larvae [9]. To understand the mechanism by which information regarding tumor is transmitted to the FB, we first examined whether more circulating hemocytes were associated with the FB in mutant larvae. We scored the circulating hemocytes labeled with GFP on the FB in mutant (*mxc^{mbn1}/Y; He>GFP*) (Figure 1b) and control (*w/Y; He>GFP*) (Figure 1a) larvae, and converted the average cell number in each larva to that in a 1 mm^2 of the FB area. In total, 61.9 hemocytes on average (n = 25) were observed in 1 mm^2 of the FB area in *mxc^{mbn1}* larvae, whereas 1.1 hemocytes (n = 22) were observed in the same FB area in normal larvae (Figure 1a, b). The differences were significant (p <0.0001, Welch's t-test) (Figure 1c). 60-fold more hemocytes were localized on the FB in mutant larvae bearing LG tumors than in control larvae. As 4-fold more hemocytes were contained in the hemolymph of mutant (7.7 ± 1.1 × 10^4 cells in 1 mL of hemolymph, n = 16) than of control (1.8 ± 0.1 × 10^4 cells in 1 mL of hemolymph, n = 12) larvae, mutant hemocytes were recruited more efficiently to the FB.

To clarify whether normal circulating hemocytes are also recruited to the FB in mutant larvae, we transplanted larval hemolymph containing GFP-labeled normal hemocytes (*w/Y;He>GFP*) into control and mutant larvae at the third-instar stage. 15 h after the transplantation of hemolymph, in which 1.2 × 10^4 circulating hemocytes (*w/Y;He>GFP*) were contained on average (n = 21) (Figure 1d, e), we counted the number of transplanted GFP+ hemocytes on the FB and converted it to the number of cells per unit area (1 mm^2) of the tissues. We scored 4.0 hemocytes on average (n = 31) per FB area in *mxc^{mbn1}* larvae (Figure 1e, f), whereas 1.5 hemocytes (n = 31) were in the same area in normal larvae (Figure 1d, f). The increase in mutant larvae was significant (p < 0.01, Welch's t-test). Confocal microscopy observation confirmed that the transplanted normal hemocytes were associated with the surface, but not the inside, of the FB in normal and mutant larvae (see the images only for reviewing in a repository).

 doi:10.20944/preprints202410.0708.v1

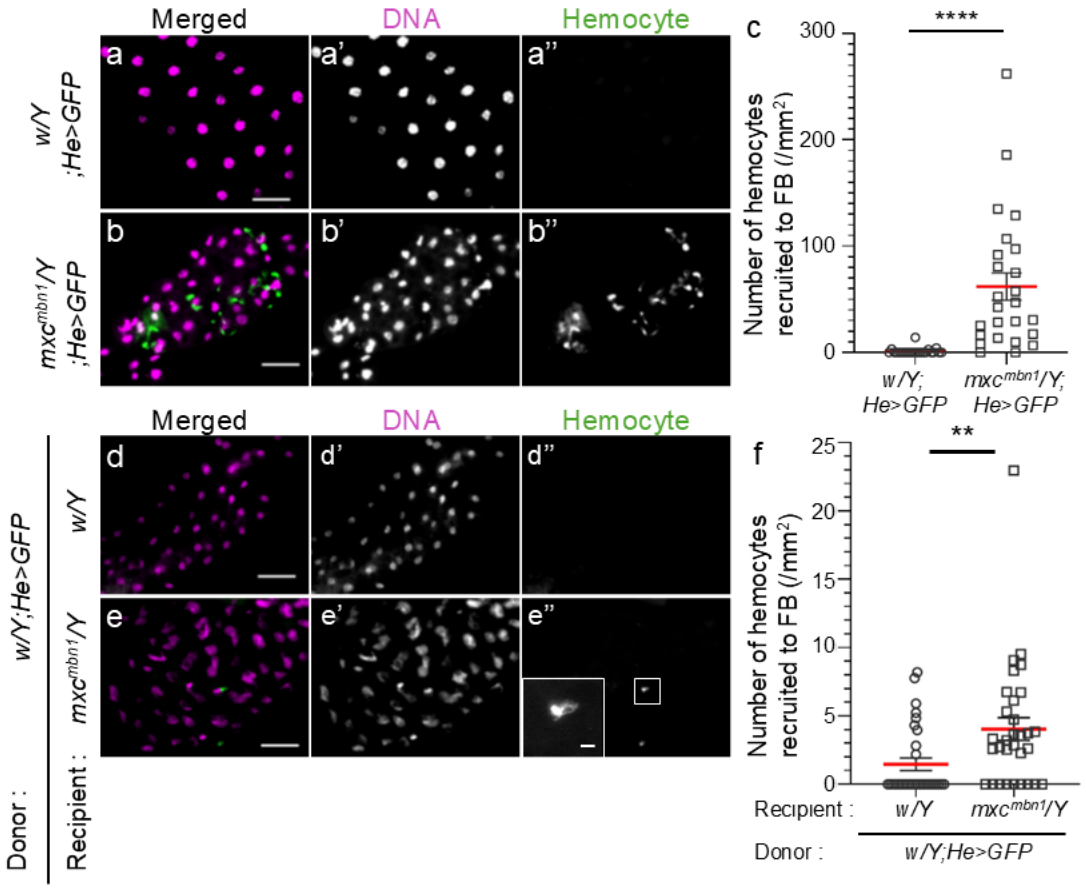

Figure 1. Hemocytes localized on the fat body (FB) in control and *mxc*^{mbn1} mutant larvae, and normal hemocytes transplanted from control larvae on the FB in control and *mxc*^{mbn1} larvae.

(a, b) Fluorescence images of circulating hemocytes labeled by GFP on the DAPI-stained FB in normal control (*w/Y;He>GFP*)(a) and *mxc*^{mbn1} (*mxc*^{mbn1}*/Y;He>GFP*)(b) larvae. The circulating hemocytes are visualized in green in a and b (white in a" and b"). DNA is stained in magenta in a and b (white in (a' and b'). Scale bars:100 μm. (c) Quantification of the number of hemocytes localized on the FB. The average number of hemocytes per unit area (mm^2) of FB was calculated. (n = 22 (*w/Y;He>GFP*), n = 25 (*mxc*^{mbn1}*/Y;He>GFP*), Welch's *t*-test, ****p<0.0001). The red line indicates the mean value; error bars indicate the standard error of the mean (SEM). (d, e) Fluorescence images of normal circulating hemocytes labeled by GFP (*w; He>GFP*), which were transplanted from control larvae on the DAPI-stained FB in (d) normal control (*w/Y*) and (e) *mxc*^{mbn1} mutant (*mxc*^{mbn1}*/Y*) larvae. The transplanted normal hemocytes are visualized in green in d and e (white in d", e"). DNA is stained in magenta in d and e (white in d' and e'). Scale bars:100 μm. (f) Quantification of the number of hemocytes localized on the FB. The average number of hemocytes per unit area of FB was calculated (n = 31 (*w/Y;He>GFP*) , n = 31 (*mxc*^{mbn1}*/Y;He>GFP*). Welch's *t*-test, **p<0.01). The red line indicates the mean value; error bars indicate the SEM.

2.2. Ectopic upd3 Expression in Normal Hemocytes Transplanted into mxc^{mbn1} *Larvae and Hemocyte-Specific Depletion of upd3 Resulted in Reduced TotF mRNA Levels and Increased LG Tumor Growth*

To clarify the possibility that hemocytes activate the JAK/STAT signaling pathway in the FB via Upd3, we initially observed ectopic *upd3* expression in normal hemocytes transplanted into *mxc*^{mbn1} larvae. We transplanted normal hemocytes harboring the *upd3-LacZ* reporter that monitors gene expression (*w/Y;He>GFP/upd3-LacZ*) into control and *mxc*^{mbn1} larvae at the third-instar stage. 15 h after transplantation, we observed a few anti-β-gal immunostaining signals above the background level (n

Preprints.org (www.preprints.org) | NOT PEER-REVIEWED | Posted: 10 October 2024 doi:10.20944/preprints202410.0708.v1

= 73 cells examined) (Figure 2a, a"'). In contrast, we observed a robust immunostaining signal in GFP+ normal hemocytes in *mxc*^{mbn1} larvae (n = 108 cells examined) (Figure 2b, b"'). The difference between control and mutant larvae was significant (p <0.0001, Welch's t-test)(Figure 2c).

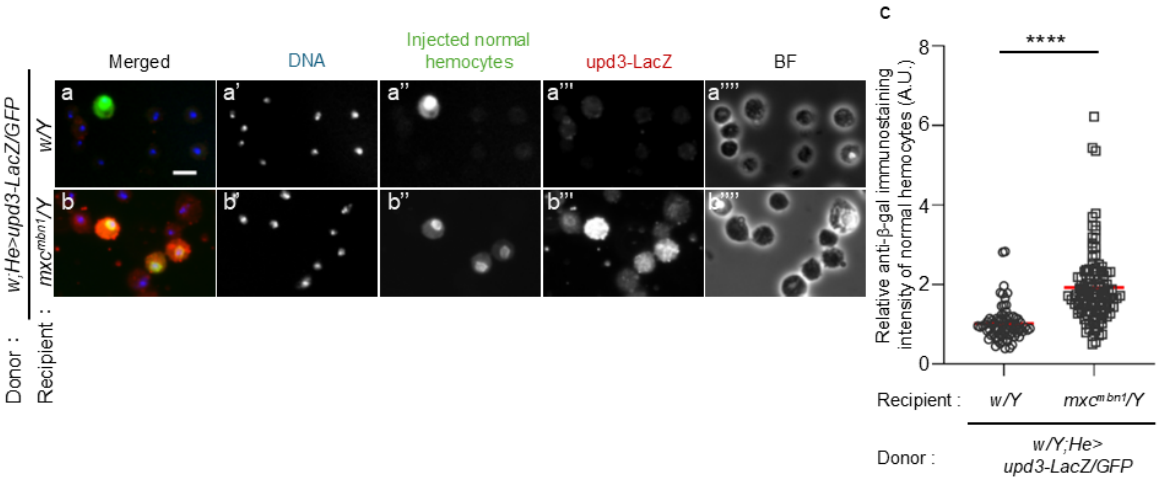

Figure 2. Ectopic expression of *upd3* gene in the normal circulating hemocytes transplanted into control and *mxc*^{mbn1} larvae by quantifying the expression using the *upd3-LacZ* reporter.

(a, b) Anti-β-gal immunostaining of the circulating hemocytes transplanted from normal larvae at mature third instar stage in normal (*w*/*Y*) (a) and *mxc*^{mbn1} (b) larvae (*mxc*^{mbn1}/*Y*). Scale bar: 10 μm; blue, DNA (white in a', b'); green, transplanted hemocytes labeled by GFP fluorescence (white in a", b") (*w*/*Y*;*He>GFP*/*upd3-LacZ*); red, anti-β-gal immunostaining to monitor the *upd3* expression (white in a"', b"'). BF, Brightfield microscopy image in a"", b"". (c) The relative fluorescence intensity of anti-β-gal immunostaining. The fluorescence intensity of each transplanted hemocyte was quantified and displayed on the y-axis relative to the fluorescence intensity of the normal control set at 1. X-axis from left to right: normal control (*w*/*Y*) (n = 73), *mxc*^{mbn1} (*mxc*^{mbn1}/*Y*) (n = 108), The average fluorescence intensity is shown as a red line. (Welch's t test, ****p < 0.0001). Error bars indicate standard error of the mean (SEM).

We investigated whether depletion of *upd3* affected *TotF* expression in the FB of *mxc*^{mbn1} larvae (Figure 3). We quantified *TotF* mRNA levels by qRT-PCR using RNAs from normal control larvae (*w*/*Y*), *mxc*^{mbn1} larvae expressing hemocyte-specific dsRNA against *GFP* mRNA (*mxc*^{mbn1}/*Y*;*He>GFPRNAi*) as a control for depletion, and *mxc*^{mbn1} larvae expressing hemocyte-specific *upd3* depletion (*mxc*^{mbn1}/*Y*;*He>upd3RNAi*). The *TotF* level in *mxc*^{mbn1} larvae with hemocyte-specific *upd3* depletion was reduced to 55.9 % of that in *mxc*^{mbn1} larvae without the depletion (Figure 3). This difference was significant (p < 0.05, one-way analysis of variance (ANOVA) with Bonferroni correction).

 doi:10.20944/preprints202410.0708.v1

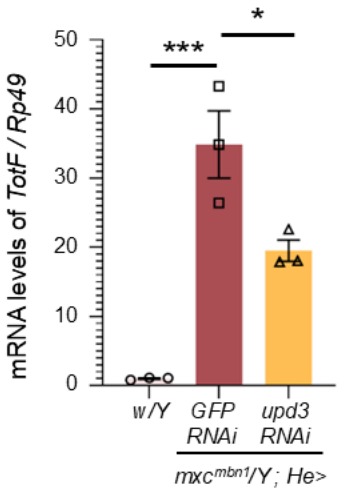

Figure 3. Reduction of mRNA levels of *TotF* in the circulating hemocytes of *mxc*^{mbn1} harboring of *upd3* depletion.

Quantification of mRNA levels of *TotF* in the FB of mature third-instar larvae by qRT-PCR. X-axis from left to right: normal control (*w*/*Y*), hemocyte-specific expression of dsRNA against GFP mRNA in *mxc*^{mbn1} mutant larvae (*mxc*^{mbn1}*/Y;He>GFPRNAi*), *mxc*^{mbn1} with hemocyte-specific depletion of *upd3* (*mxc*^{mbn1}*/Y;He>upd3RNAi*); Y-axis shows mRNA levels of the target gene (*TotF*) relative to the endogenous control gene (*Rp49*). (One-way ANOVA with Bonferroni correction. *$p < 0.05$, ***$p < 0.001$ n = 3). Bars indicate mean mRNA levels of the target gene (mean of three quantification data) and error bars indicate the SEM.

We further investigated whether *upd3* depletion in hemocytes influences the hyperplasia of LG tumors in *mxc*^{mbn1} larvae. The average LG sizes of the normal control, *mxc*^{mbn1} larvae (*mxc*^{mbn1}*/Y;He>GFPRNAi*), and *mxc*^{mbn1} larvae harboring the *upd3* depletion (*mxc*^{mbn1}*/Y;He>upd3RNAi*) were 0.04 mm^2 (n = 20), 0.36 mm^2 (n = 20), and 0.53 mm^2 (n = 17), respectively (Figure S1d). The LG size of *mxc*^{mbn1} with *upd3* depletion (*mxc*^{mbn1}*/Y;He>upd3RNAi*) was more than 1.4-fold higher than that of *mxc*^{mbn1} (*mxc*^{mbn1}*/Y;He>GFPRNAi*). This difference was significant ($p < 0.0001$, one-way ANOVA with Bonferroni correction).

2.3. Hyper-Activation of JNK in Normal Hemocytes Transplanted into mxc^{mbn1} *Larvae and Its Role in Inducing TotF Expression and Suppressing Tumor Growth*

We next investigated whether the JNK pathway was activated in normal hemocytes transplanted into *mxc*^{mbn1} larvae. 15 h after the transplantation of the normal hemocytes (1.2×10^4 cells) (*w/Y;He>GFP*) into normal larvae (*w*/*Y*), we detected only a few immunostaining signals with the anti-phosphorylated JNK antibody over the background level in GFP+ transplanted cells (n = 88 cells examined) (Figure 4a‴). In contrast, we observed a strong immunostaining signal in GFP+ normal hemocytes in the hemolymph of *mxc*^{mbn1} larvae (n = 96 cells) (Figure 4b‴). The differences in the signal intensity corresponding to the extent of the JNK activation between the control and mutant larvae were significant (Figure 4c). Moreover, MMP1, another downstream target of the JNK pathway, was also induced in normal hemocytes transplanted into mutant larvae (Figure S2).

 doi:10.20944/preprints202410.0708.v1

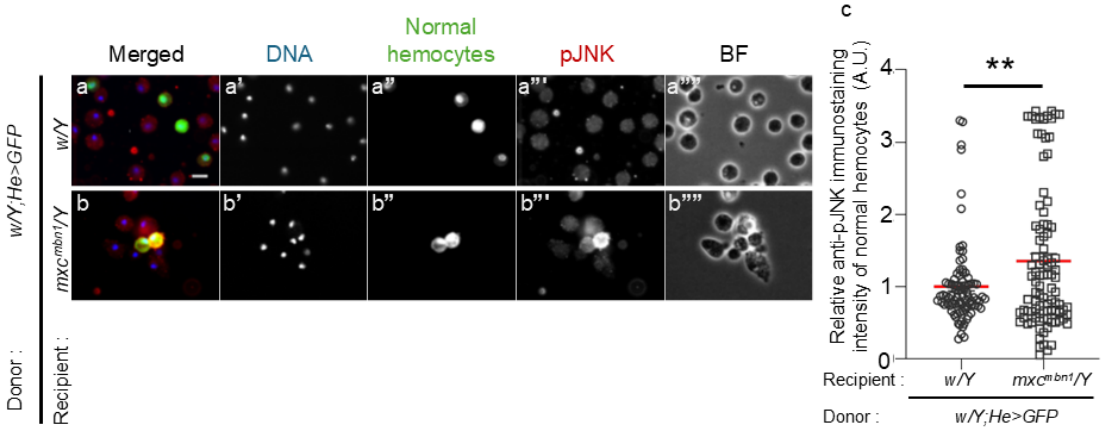

Figure 4. Anti-phosphorylated JNK (pJNK) immunostaining of the normal circulating hemocytes transplanted into control and *mxc*^{mbn1} larvae to detect activation of the JNK pathway.

(a, b) Fluorescence images of circulating hemocytes transplanted from normal larvae (*w*/*Y*;*He>GFP*) in normal (*w*/*Y*) (a) and *mxc*^{mbn1} larvae (*mxc*^{mbn1}/*Y*) (b). Scale bar: 10 μm; blue, DNA (white in a′, b′); green, transplanted hemocytes (white in a″, b″); red, the hemocytes harboring the activated JNK (pJNK) (white in a‴, b‴). BF, Brightfield microscopy image in a⁗, b⁗. (c) The relative fluorescence intensity of anti-pJNK immunostaining. The fluorescence intensity of each transplanted hemocyte was quantified and displayed on the y-axis relative to the fluorescence intensity of the normal control set at 1. X-axis from left to right: normal control (*w*/*Y*) (n = 88), *mxc*^{mbn1} (*mxc*^{mbn1}/*Y*) (n = 96) larvae, The average fluorescence intensity is shown as a red line. (Welch's *t* test, $^{**}p < 0.01$). Error bars indicate the SEM.

As the JNK pathway can induce the expression of Upd3 during development [26], we next investigated whether the induction of *TotF* expression in the FB depended on the JNK pathway in the hemocytes of *mxc*^{mbn1} larvae. First, we examined whether the JNK pathway was activated to induce *TotF* expression in the FB of normal control larvae (*w*/*Y*) and *mxc*^{mbn1} larvae expressing control dsRNA against *GFP* mRNA (*mxc*^{mbn1}/*Y*;*He>GFPRNAi*), the mutant larvae harboring the hemocyte-specific *hep* depletion (*mxc*^{mbn1}/*Y*;*He>hepRNAi*) and those harboring *bsk* depletion (*mxc*^{mbn1}/*Y*;*He>bskRNAi*). The *TotF* mRNA levels in *mxc*^{mbn1} with the hemocyte-specific depletion of *hep* and *bsk* were reduced to an average of 39.6% and 24.3% of those in *mxc*^{mbn1}, respectively (Figure 5a, b). This difference was significant ($p < 0.01$, Figure 5a; $p < 0.001$, Figure 5b; one-way ANOVA with Bonferroni correction).

We further investigated whether the depletion of JNK in the hemocytes of *mxc*^{mbn1} larvae enhanced the hyperplasia of LG tumors (Figure 5c-g). The average LG size of normal control (*w*/*Y*) and *mxc*^{mbn1} (*mxc*^{mbn1}/*Y*; *He>GFPRNAi*) larvae at the third instar stage was 0.04 mm^2 (n = 20) and 0.39 mm^2 (n = 20), respectively. The LGs of *mxc*^{mbn1} were more than 12-fold higher on average than those of the controls (Figure 5g). LG sizes further increased in *mxc*^{mbn1} larvae harboring the hemocyte-specific depletion *hep* (*mxc*^{mbn1}/*Y*; *He>hepRNAi*) and those harboring the depletion of *bsk* (*mxc*^{mbn1}/*Y*; *He>bskRNAi*) to 0.48 mm^2 (n = 19) and 0.50 mm^2 (n = 33), respectively (Figure 5e, f). These differences from LG sizes of *mxc*^{mbn1} larvae without these depletions were significant ($p < 0.01$, $p < 0.001$, one-way ANOVA with Bonferroni correction) (Figure 5g).

Preprints.org (www.preprints.org) | NOT PEER-REVIEWED | Posted: 10 October 2024 doi:10.20944/preprints202410.0708.v1

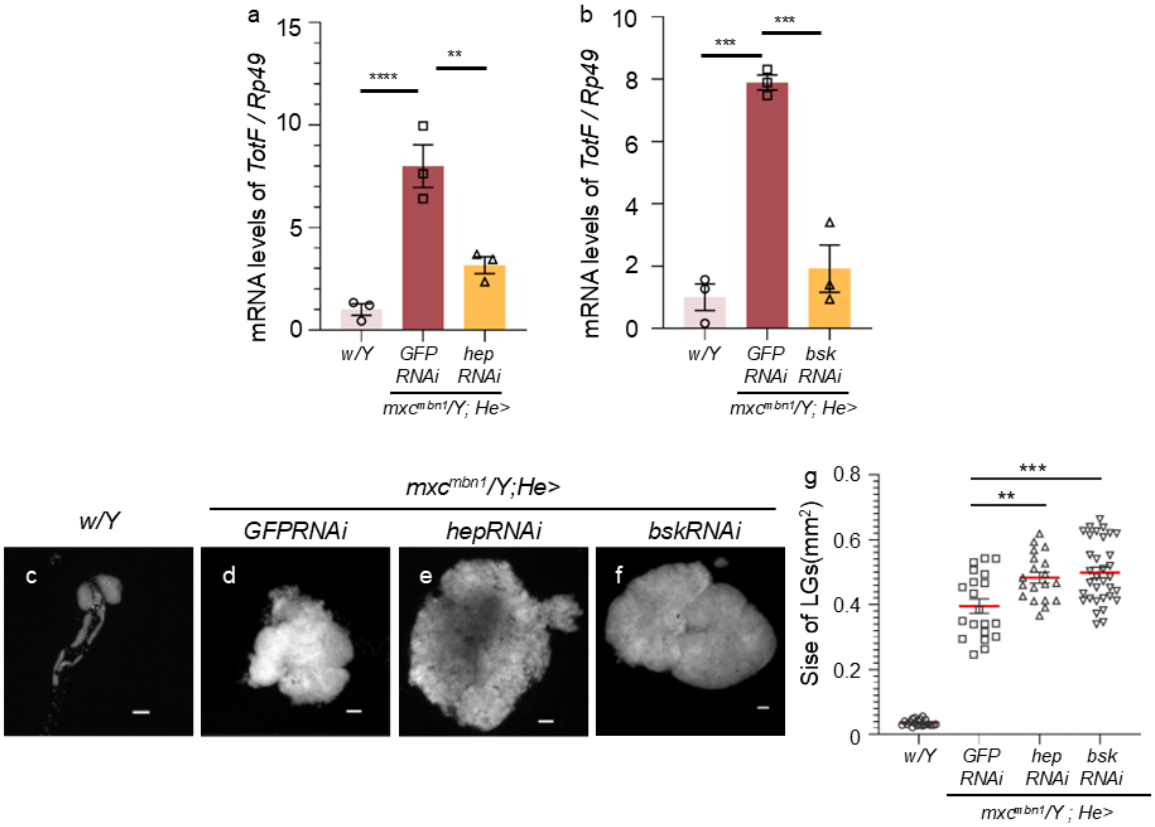

Figure 5. Reduced *TotF* mRNA levels in the FB of *mxc*^{mbn1} larvae harboring circulating hemocyte-specific depletion of JNK pathway's components, JNKK encoded by *hep* and JNK by *bsk*.

(a, b) Quantification of *TotF* mRNA levels in the FB of mature third instar larvae by qRT-PCR. X axis from left to right: normal control (*w*/*Y*), *mxc*^{mbn1} expressing control dsRNA against *GFP*dsRNAs specifically in hemocytes (*mxc*^{mbn1}*/Y; He>GFPRNAi*), and hemocyte-specific depletion of *JNKK* (*hep*) in *mxc*^{mbn1} (*mxc*^{mbn1}*/Y;He>hepRNAi*) (a) or hemocyte-specific depletion of *JNK* (*bsk*) in *mxc*^{mbn1} (*mxc*^{mbn1}*/Y;He>bskRNAi*) (b). The y-axis shows the mRNA levels of the target gene (*TotF*) relative to the endogenous control gene (*Rp49*). One-way ANOVA with Bonferroni correction, $^{**}p < 0.01$, $^{***}p < 0.001$, $^{****}p < 0.0001$ n = 3. Bars indicate relative mRNA levels of the target gene (mean of three quantification data), and error bars indicate the SEM. (c-f) DAPI-stained images of LGs from mature third instar larvae. (c) normal control (*w*/*Y*); (d) *mxc*^{mbn1} mutant control (*mxc*^{mbn1}*/Y;He>GFPRNAi*); (e) *mxc*^{mbn1} mutant larvae with hemocyte-specific *hep* depletion (*mxc*^{mbn1}*/Y;He>hepRNAi*); (f) *mxc*^{mbn1} mutant larvae with hemocyte-specific *bsk* depletion (*mxc*^{mbn1}*/Y;He>bskRNAi*) Scale bar is 100 μm. (g) Quantification of the LG sizes. From left to right: normal control (*w*/*Y*), *mxc*^{mbn1} expressing hemocyte-specific dsRNA against *GFP* mRNA (*mxc*^{mbn1}*/Y;He>GFPRNAi*), *mxc*^{mbn1} harboring hemocyte-specific *hep* depletion (*mxc*^{mbn1}*/Y;He>hepRNAi*) and *mxc*^{mbn1} harboring hemocyte-specific *bsk* depletion (*mxc*^{mbn1}*/Y;He>bskRNAi*). One-way ANOVA with Bonferroni correction, $^{**}p < 0.01$, $^{***}p < 0.001$, n = 20 (*w*/*Y*), n = 20 (*mxc*^{mbn1}*/Y;He>GFPRNAi*), n = 19 (*mxc*^{mbn1}*/Y;He>hepRNAi*), n = 33 (*mxc*^{mbn1}*/Y;He>bskRNAi*). Red lines indicate means and error bars indicate the SEM.

2.4. Ectopic Expression of Eiger, a TNF Superfamily Ligand, in LG Tumors of mxc^{mbn1} *Mutant Larvae*

To understand the mechanism by which the activation of the JNK pathway occurs in hemocytes, leading to *TotF* induction in the FB, we investigated whether Eiger is involved in JNK activation in *mxc*^{mbn1} larvae. We examined Eiger expression in the LG tumors of the mutant larvae by immunostaining with an anti-Eiger antibody (Figure 6a, b). The average fluorescence intensity of whole lobe regions of LGs was calculated from immunostaining images of LGs from control (*w*/*Y*) and *mxc*^{mbn1} (*mxc*^{mbn1}*/Y*) larvae at the third-instar stage. The average fluorescence intensity was 5-fold

 doi:10.20944/preprints202410.0708.v1

higher in mutant LGs (n = 50) than in normal control LGs (n = 42). This difference was significant (p <0.0001, Welch's t-test) (Figure 6c). These results indicated that Eiger expression was considerably higher in LG tumors of *mxc*^{mbn1} than in control LGs.

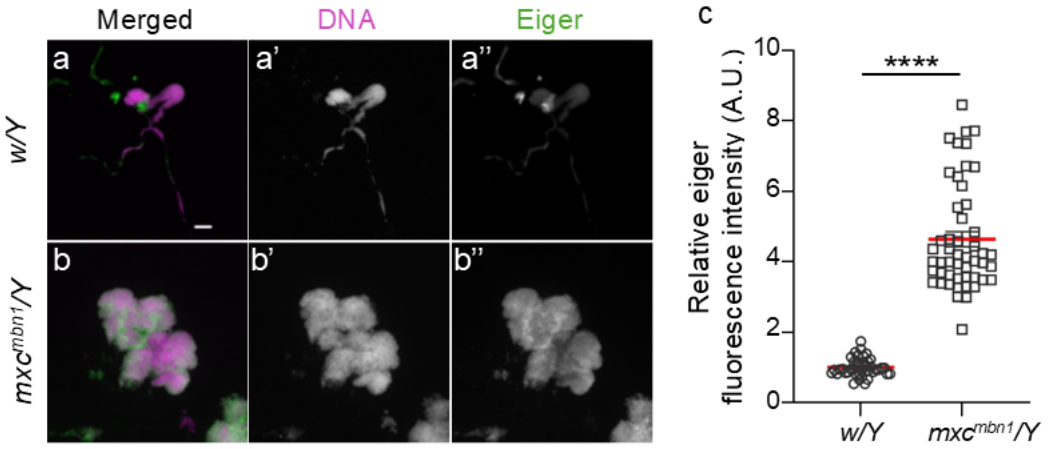

Figure 6. Increased expression of Eiger in the LGs of *mxc*^{mbn1} larvae, compared to that of normal LGs.

(a, b) Fluorescence images of the LGs from mature third instar larvae immunostained with anti-Eiger antibody. a represents normal control (*w*/*Y*) and b represents LG of *mxc*^{mbn1} larvae (*mxc*^{mbn1}/*Y*). Scale bar is 100 μm; magenta indicates DNA staining (white in a', b') and green indicates antibody staining signal (white in a", b"). (c) Quantification of fluorescence intensity in anti-Eiger immunostaining of LG in control and *mxc*^{mbn1} larvae. Relative values are shown on the Y-axis with the mean fluorescence intensity of the normal control as 1. From left to right, the X-axis shows the fluorescence intensity in LGs of normal control (*w*/*Y*), *mxc*^{mbn1} larvae (*mxc*^{mbn1}/*Y*). Welch's t-test, ****p < 0.0001, n = 42 (*w*/*Y*), n = 50 (*mxc*^{mbn1}/*Y*). Error bars indicate the SEM.

2.5. Depletion of the Eiger Receptors in Circulating Hemocytes Resulted in the Inhibition of TotF Induction in the FB and Enhancement of LG Tumor Growth in mxc^{mbn1}

To address the mechanism by which the JNK pathway is activated in hemocytes, we investigated whether Eiger receptors on hemocytes are required for *TotF* induction in the FB of mutant larvae. Eiger binds to two types of receptors encoded by *wgn* and *grnd*, which commonly activate the JNK pathway to induce *upd3* transcription. We quantified the *TotF* mRNA levels in *mxc*^{mbn1} larvae harboring hemocyte-specific depletion of *wgn* (*mxc*^{mbn1}*/Y;He>wgnRNAi*) or *grnd* (*mxc*^{mbn1}*/Y;He>grndRNAi*). We performed qRT-PCR using total RNA prepared from normal, *mxc*^{mbn1}, and mutant larvae harboring these depletions. The hemocyte-specific depletion of *wgn* and *grnd* in *mxc*^{mbn1} resulted in reduced mRNA levels of 17.1% and 20.0% of those in *mxc*^{mbn1} larvae, respectively (Figure 7). These differences were significant (p <0.0001, one-way ANOVA with Bonferroni correction).

Preprints.org (www.preprints.org) | NOT PEER-REVIEWED | Posted: 10 October 2024 doi:10.20944/preprints202410.0708.v1

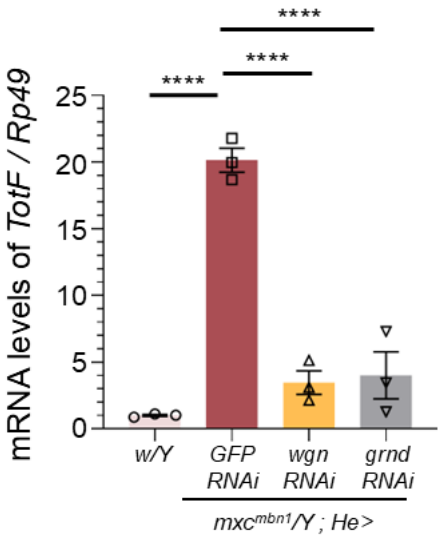

Figure 7. A reduction of *TotF* mRNA levels in circulating hemocytes harboring depletion of *wgn* or *grnd* in *mxc*^{mbn1} larvae.

Quantification of the *TotF* mRNA levels in the FB of mature third instar larvae with circulating hemocytes harboring depletion of receptor components (Wgn and Grnd) by qRT-PCR. X-axis from left to right: normal control (*w*/*Y*), *mxc*^{mbn1} larvae hemocyte-specific expression of dsRNA against *GFP* mRNA (*mxc*^{mbn1}*/Y;He>GFPRNAi*), and *mxc*^{mbn1} larvae with hemocyte-specific depletion of *wgn* (*mxc*^{mbn1}*/Y;He>wgnRNAi*), *mxc*^{mbn1} with the depletion of *grnd* (*mxc*^{mbn1}*/Y;He>grndRNAi*). The y-axis shows the mRNA levels of *TotF* relative to the endogenous control gene (*Rp49*). Bars indicate relative mRNA levels of the target gene (mean of triplicate quantification data), and error bars indicate the SEM. ****p <0.0001, One-way ANOVA with Bonferroni correction.

We quantified the LG size in normal (*w*/*Y*), *mxc*^{mbn1} larvae (*mxc*^{mbn1}*/Y;He>GFPRNAi*), and those harboring depletion of *wgn* or *grnd* genes encoding one of the Eiger receptors (Figure S3a-e). The average LG size of normal and *mxc*^{mbn1} larvae was 0.04 mm^2 (n = 20) and 0.39 mm^2 (n = 20), respectively. In contrast, the average LG sizes of *mxc*^{mbn1} larvae harboring the hemocyte-specific depletion of *wgn* and those harboring the *grnd* depletion were 0.51 mm^2 (n = 19) and 0.45 mm^2 (n = 42), respectively (Figure S3f). Their LG sizes were 1.3- and 1.1-fold larger than those of *mxc*^{mbn1} without RNAi, respectively. These differences were significant (p < 0.001 and p < 0.05, one-way ANOVA with Bonferroni correction).

2.6. TotB and F Proteins Induced in the FB were Incorporated into Transplanted Normal Hemocytes in mxc^{mbn1} *Larvae But Not in Those in Control Larvae*

The Tot proteins produced in the FB have an antitumor effect on LG tumors in *mxc*^{mbn1} larvae [13]. Thus, we next investigated the mechanisms by which Tot proteins exert tumor-specific effects. TotB and TotF proteins are incorporated into circulating hemocytes in mutant larvae. To exclude the possibility that these phenotypes may reflect the characteristics of mutant tumor cells, we confirmed whether normal hemocytes transplanted from control larvae incorporated these Tot proteins. We transplanted normal circulating hemocytes (1.2 × 10^4 hemocytes on average) expressing GFP from control larvae (*w/Y;He>GFP*) into mutant larvae in which HA-tagged TotB (*mxc*^{mbn1}*/Y;r4>TotB-HA*) or TotF (*mxc*^{mbn1}*/Y;r4>TotF-HA*) were expressed in their FB. 15 h after transplantation, we performed anti-HA immunostaining of circulating hemocytes in *mxc*^{mbn1} larvae. We observed a distinctive immunostaining signal for TotB in the cytoplasm of 40.4% of GFP+ hemocytes (*w/Y;He>GFP*) in *mxc*^{mbn1} larvae (n = 9 cells out of 23 cells) (Figure 8b'', 8e), whereas we found fewer hemocytes showing TotB signal, whose intensity was slightly above the background level (9.8% of GFP+ hemocytes) in control larvae (*w/Y; r4>TotB-3HA*) (n = 39 cells) (Figure 8a'', 8e). The difference was statistically significant (p < 0.05, Figure 8e). Consistently, 56.7% of circulating hemocytes in *mxc*^{mbn1} larvae showed

 doi:10.20944/preprints202410.0708.v1

a distinctive anti-HA immunostaining signal for TotF (n = 9 cells out of 16 cells) (Figure 8d'', 8e). The difference was statistically significant ($p < 0.001$, Figure 8e).

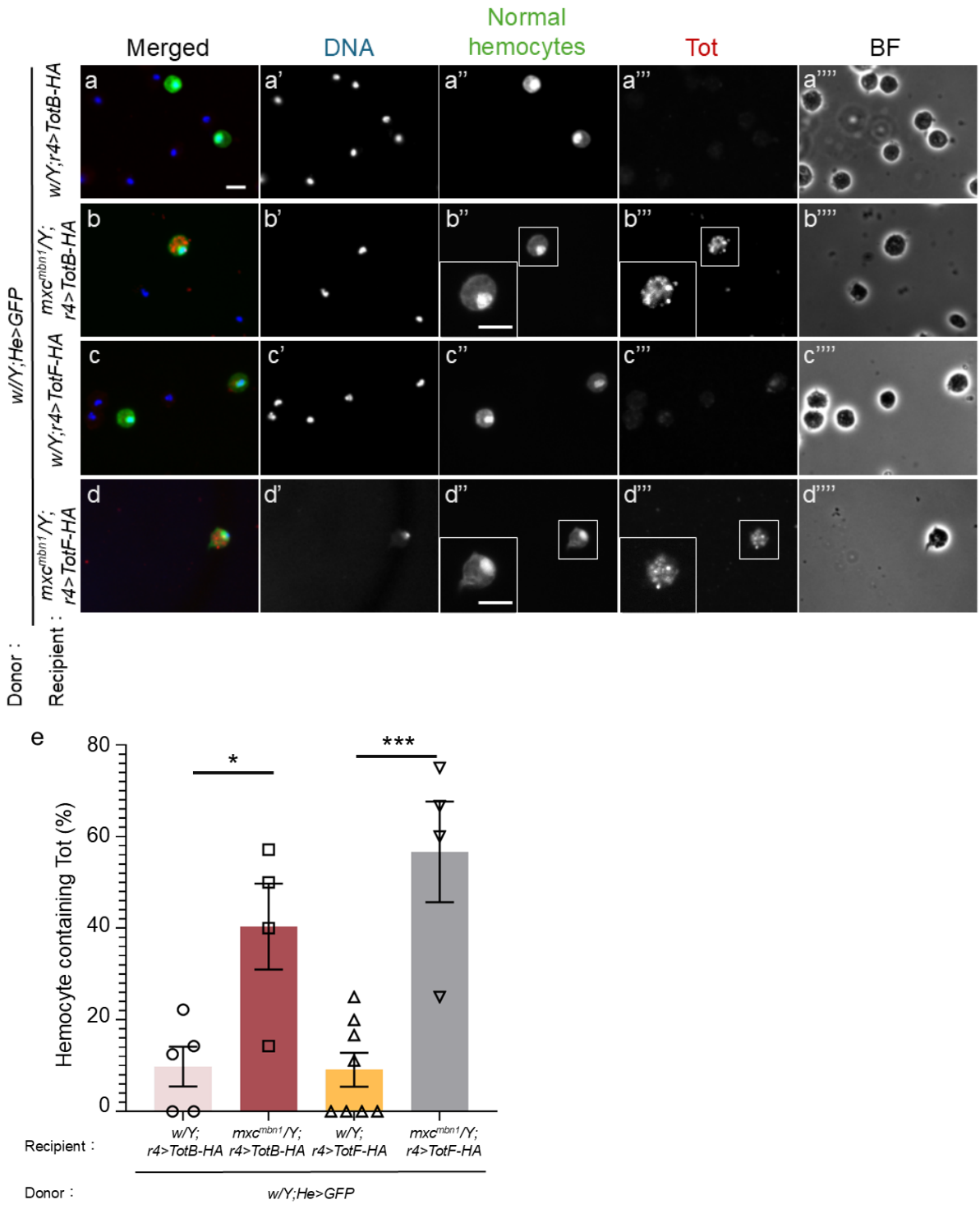

Figure 8. Uptake of TotB and TotF proteins into transplanted normal hemocytes in *mxc*^{mbn1} larvae.

(a-d) Anti-HA immunostaining of circulating hemocytes to detect HA-tagged TotB (a, b) and TotF (c, d), induced in the FB in normal control larvae (*w/Y; r4>TotB-HA*) (a), (*w/Y; r4>TotF-HA*) (c), and *mxc*^{mbn1} larvae (*mxc*^{mbn1}*/Y; r4>TotB-HA*) (b), and (*mxc*^{mbn1}*/Y; r4>TotF-HA*) (d). The same hemolymph volume containing circulating hemocytes from control larvae (*w; He>GFP*) was transplanted into the mutant larvae. The transplanted normal hemocytes labeled by GFP fluorescence are colored in green in a-d (white in (a''–d''). Anti-HA immunostaining signal of the hemocytes is in red in a–d (white in

 doi:10.20944/preprints202410.0708.v1

(a‘‘‘–d‘‘‘). DNA is blue in a–d (white in a‘–d‘). Magnified images of the hemocytes are presented in the insets in b“, b“‘, and d“, d“‘. All scale bars represent 10 μm. (e) Percentages of normal hemocytes containing TotB or TotF proteins induced in the FB in control and *mxc*^{mbn1} mutant larvae. X-axis from left to right: normal control larvae in which HA-tagged TotB was ectopically expressed in the FB of *w/Y; r4>HA-TotB*, *mxc*^{mbn1} */Y; r4>HA-TotB*, *w/Y; r4>HA-TotF*, and *mxc*^{mbn1} */Y; r4>HA-TotF* larvae. Bars indicate the average frequencies of GFP+ hemocytes containing TotB or TotF, and error bars indicate SEM. **p* <0.05, ****p* <0.001, One-way ANOVA with Bonferroni correction.

2.7. Normal Hemocytes Containing TotF were Closely Associated with the LGs in mxc^{mbn1} *Larvae But Not in Normal Larvae*

To clarify the hypothesis that hemocytes incorporating Tot proteins secreted from the FB would be recruited and release the antitumor proteins toward the LG tumor, we investigated whether TotF was incorporated into transplanted normal hemocytes and associated with the LG tumor in *mxc*^{mbn1} larvae. We transplanted normal hemocytes (1.4×10^4 cells of *w/Y;He>GFP*) in mutant larvae expressing either of the HA-tagged Tot proteins in their FB (*mxc*^{mbn1}*/Y;r4>TotB-HA*, or *mxc*^{mbn1}*/Y;r4>TotF-HA*). 15 h after transplantation, we collected the mutant LGs and examined whether the hemocytes closely associated with LG tumors contained Tots by anti-HA immunostaining. Among transplanted normal hemocytes, 22.2 % of the GFP+ hemocytes contained Tot proteins in the cytoplasm (Figure 9b‘‘‘, c‘‘‘) . In contrast, we did not find any hemocytes containing Tot proteins on the LGs in the control larvae after transplanting the same hemolymph volume from the control larvae (Figure 9a‘‘‘).

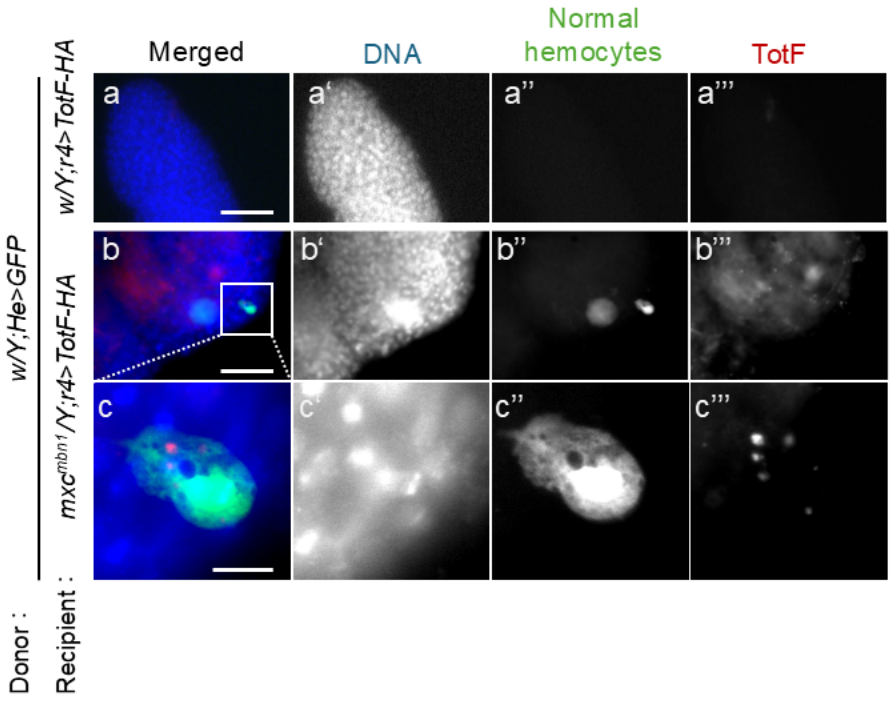

Figure 9. The transplanted normal hemocytes on the LG tumor incorporated the TotF protein that expressed in the FB in *mxc*^{mbn1} larvae.

(a-c) Anti-HA immunostaining of normal circulating hemocytes expressing GFP transplanted from normal larvae (*w/Y;He>GFP*) on the LG lobes to detect HA-tagged TotF in control (a) and *mxc*^{mbn1} (b, c) larvae. A transplanted hemocyte enclosed by a square in (b) is magnified in (c). The transplanted hemocytes are in green in a-c (white in a“–c“). Anti-HA immunostaining signal (Tot) corresponding the TotF signal is in red in a-c (white in a‘‘‘-c‘‘‘). The PC cells have a property that incorporates the Tot-HA proteins. DNA is colored in blue in a-d (white in (a‘-c‘)). The weak blue signal around the hemocyte in c represents DNA staining of the LG cells on which the hemocyte was localized. Scale bars in a, c and b represent 50 μm and 10 μm, respectively.

 doi:10.20944/preprints202410.0708.v1

3. Discussion

In *mxc*^{mbn1} mutant larvae, the hemocyte precursor cells in the LG show malignant tumor phenotypes. In response to the tumor, the JAK/STAT pathway is activated in the FB, thereby inducing Tot family proteins with antitumor activity. However, the mechanism by which this induction occurs remained unclear prior to this study. We found that many hemocytes were recruited to the LG tumor and FB in the mutant larvae. Transplanting normal hemocytes into mutant larvae also resulted in efficient recruitment. Thus, we hypothesized that hemocytes recruited to the FB convey tumor information from the LG tumor. The induction of TotA, B, C, and F in mutant FB depends on the activation of the JAK/STAT pathway [13]. We addressed the mechanism of pathway activation in the FB separated from the LG tumor. Upd3, a functional ortholog of the mammalian IL-6 cytokine [27], was ectopically expressed in the hemocytes of *mxc*^{mbn1} larvae. Depletion of *upd3* in hemocytes decreased *TotF* mRNA levels in the FB of mutant larvae, which eventually resulted in the enhancement of LG tumor growth. These genetic data indicate that the ectopic *upd3* expression in hemocytes is required for *TotF* induction in FB and the LG tumor suppression. Second, we examined the mechanism by which *upd3* was induced in hemocytes. Eiger, which corresponds to the mammalian TNF cytokines [28], was highly expressed in LG tumors. We depleted mRNAs encoding Eiger receptors and signaling factors that constitute the JNK pathway in hemocytes. In every case, *TotF* mRNA levels in the FB were reduced and tumor growth was increased, indicating that the activation of the JNK pathway in hemocytes is required to suppress LG tumor in *mxc*^{mbn1} larvae. Third, we also examined how Tots selectively exhibit antitumor effects. TotB and TotF were incorporated into circulating hemocytes, and the cells containing the Tots were recruited to the tumors.

3.1. Signal Transfer from the LG Tumor toward the FB via Circulating Hemocytes Expressing Upd3

In *mxc*^{mbn1} larvae carrying the LG tumor, the JAK/STAT pathway in the FB is activated to induce tumor suppressor *Tot* genes [13]. However, to activate the pathway in FB distant from the tumor, information relevant to the tumor must be conveyed to the FB in which antitumor proteins are produced. Transplanted normal hemocytes are efficiently recruited to LG tumors in *mxc*^{mbn1} larvae [9]. Moreover, the present study showed that many mutant and normal hemocytes were recruited to the FB of *mxc*^{mbn1} larvae. The binding of Upd3 to its receptor domain activates the JAK/STAT signaling pathway [11]. Based on these findings, hemocytes on the tumor may have been recruited to the FB through the hemolymph after tumor recognition. Therefore, the information is transmitted to the FB. Consequently, the JAK/STAT pathway may be activated in FB. Similarly, Upd3 is ectopically expressed in the larvae bearing malignant tumors related to the loss of cell polarity [29]. These data suggest that this cytokine is involved in the activation of the innate immune pathway in the FB.

We confirmed that the ectopic expression of Upd3 in normal hemocytes transplanted into *mxc*^{mbn1} larvae required for *TotF* induction in the FB. Hemocytes may be recruited to the FB while secreting Upd3 cytokines through the hemolymph to the receptor on the FB surface. This activates the JAK/STAT pathway and promotes *TotF* expression. The pro-inflammatory cytokine IL-6 is also secreted primarily by lymphocytes and macrophages, which is consistent with findings in *Drosophila* [30]. IL-6 exerts a tumor-suppression effect on cancer cells derived from mammalian breast cancer [31]. These findings support the hypothesis that macrophage-like blood cells are involved in cancer-related signaling via cytokines, the expression of which is induced. Circulating hemocytes also accumulate on imaginal disc tumors in *Drosophila dlg* mutant larvae, and the Toll-mediated innate immune pathway is activated in the FB of mutant larvae [8]. This previous finding is consistent with our model that Upd3 in hemocytes is required to signal the FB in LG tumor-bearing larvae.

3.2. Macrophage-like Plasmatocytes May Recognize the Eiger Cytokine Secreted from LG Tumors and Convey Information on Tumor Cells to the FB

Our current data suggested that Upd3, which is ectopically induced and secreted from hemocytes, may promote the activation of the JAK/STAT pathway in the FB, whereas little Upd3 expression was observed in the normal hemocytes of tumor-free larvae. Consistently, high Upd3

 doi:10.20944/preprints202410.0708.v1

expression has been reported in the hemocytes of mutants with imaginal disc tumors [32]. Based on these findings, the Upd3 induced in hemocytes may be used as a signal to notify the FB cells of the presence of tumor cells.

We next investigated why hemocytes could recognize LG tumors. Eiger, a member of the TNF family in *Drosophila*, is highly expressed in LG tumors. Furthermore, the Eiger receptor and JNK signaling factors downstream of the receptor in hemocytes are required for *TotF* expression in the FB. Eiger binds to its receptors Wgn and Grnd and activates the JNK pathway [15]. Downstream of the JNK pathway, one of the targets, Upd3, is produced [16]. The recognition of LG tumor cells expressing Eiger via its receptors on the surface of hemocytes may promote Upd3 expression. Subsequently, these hemocytes are recruited to the FB while expressing Upd3. This induces *TotF* expression in FB. JNK is activated in the hemocytes of mxc^{mbn1} mutant larvae [9,24]. Our results confirm that the ectopic expression of Upd3 and activation of the downstream JNK pathway in hemocytes are required to induce *TotF* expression in the FB. Based on these results, plasmatocytes that accept Eiger via its receptors activate the intracellular JNK pathway. This may promote the expression of Upd3, and eventually TotF, in FB.

In cultured cells derived from mammalian breast cancer, TNF-α is a potent activator of immune cells via the induction of inflammatory cytokines such as IP-10 [33]. Increased IP-10 levels are associated with the pathology of various inflammatory disorders, including cancer. Therefore, a similar regulatory mechanism may be present in *Drosophila*, in which a TNF ortholog acts as a cytokine that mediates communication between tissues. If our model is correct, the downregulation of Eiger in LG tumors would inhibit the activation of JNK in hemocytes. This must be verified in future experiments by transplanting normal hemocytes into mutant larvae. The mechanism by which hemocytes are recruited to LG tumors also remains unclear; the induction of Eiger expression may activate the JNK pathway, which in turn leads to cell death [34]. The activation of JNK and induction of its target, Mmp1, have already been reported in LG tumors of *mxc* mutant larvae, resulting in the disassembly of the basement membrane of LG cells [9,24]. The resulting cellular fragments may be phagocytosed by macrophage-like plasmatocytes and recognized as a sign of a tissue damage. Which chemokine(s) recruit plasmatocytes to LG tumors needs to be clarified in the future.

3.3. Possible Role of Circulating Hemocytes as a Vector to Transport Secreted Antitumor Proteins, Tots, to the LG Tumor

Many circulating hemocytes and hemocytes recruited to the LG tumor internalized TotF secreted from the FB. This suggests that hemocytes act as a vector that allows Tot proteins to be selectively supplied to the tumor. Normal hemocytes transplanted into mutant larvae are also recruited to LG tumors [9] and FB (this study). TotF and TotB proteins are incorporated into the cytoplasm of circulating hemocytes and immunostaining signals for Tots are present in small vesicles in the cytoplasm of hemocytes [13]. Other AMPs, such as Drosomycin and Defensin, also exhibit antitumor activity by being incorporated into hemocytes and recruited to the LG tumor [7]. Mammalian tumor-associated macrophages (TAMs) facilitate disease progression by promoting tumor cell growth and suppressing adaptive immune responses [35]. The extent of TAM recruitment to tumors tends to correlate with poor disease prognosis [36]. Some TAMs secrete cytokines such as globule-EGF factor 8 and IL-6, which lead to the tumorigenicity of cancer stem cells [37]. Other mammalian cytokines are also consistently incorporated into the cytoplasm in vesicle-like forms [38]. Similarly, Eiger induces cell death via Rac1-dependent endocytosis [39]. Based on these observations, we speculate that *Drosophila* hemocytes may also take up Tot proteins secreted from the FB, probably via endocytosis. Subsequently, hemocytes are recruited to the tumor, where they release Tots, probably via exocytosis, for example, as observed in cytotoxic granule discharge from natural killer cells and T lymphocytes [40]. Alternatively, *Drosophila* plasmatocytes, which are equivalent to mammalian macrophages, have phagocytic functions, which may be involved in the incorporation of Tots. In the near future, identifying the factors involved in Tot dynamics will be necessary. Additionally, the mechanisms underlying the uptake and release of Tot antitumor proteins need to be clarified.

 doi:10.20944/preprints202410.0708.v1

4. Materials and Methods

4.1. Drosophila Stocks

w^{1118}, abbreviated as *w*, was used as a normal control stock . The recessive lethal allele of *mxc*, *mxc^{mbn1}* (#6360, Bloomington Drosophila Stock Center (BDSC, Indiana University, Bloomington, USA) was used [7,22]. As the *mxc* is a X-linked gene, the mutant male (*mxc^{mbn1}/Y*) and control male (*w/Y*) were used for experiments. For the depletion of JNK factors and several other proteins, we used the following *UAS-RNAi* stocks; *P{w+mC=UAS-GFP.dsRNA.R}142* (*UAS-GFPRNAi*) (BDSC, #BL9330) [13], *P{KK110348}VIE-260B* (*UAS-upd3RNAi*) (VDRC, #v106869) [41], *P{y+t7.7 v+t1.8=TRiP.HMC03962}attP40* (*UAS-wgnRNAi*) (BDSC, #BL55275) [42], *P{KK109939}VIE-260B* (*UAS-grndRNAi*) (VDRC, #104538) [43], *P{TRiP.HMC03539}attP2* (*UAS-bskRNAi*) (#53310) [44], and *P{y+t7.7 v+t1.8=TRiP.GL00089}attP2* (*UAS-hepRNAi*) (BDSC, #BL35210) [45]. *P{w[+mC]=upd3-lacZ.Z}5F* (*upd3-LacZ*) (BDSC, #BL-98418) was used to monitor the *upd3* gene expression. To induce expression of HA-tagged TotB and TotF, M{UAS-TotB.ORF.3xHA.GW}ZH-86Fb (FlyORF, Zurich, Switzerland, #002780)) and M{UAS-TotF.ORF.3 xHA.GW}ZH-86Fb (FlyORF, #00351) were used [13].Following the GAL4-driver stocks were used; *P{w+mC=He-Gal4.Z}*(BDSC, #BL8699) for induction of gene expression in circulating hemocytes [23], *P{upd3-GAL4}* (provided by N. Perrimon, Harvard Medical School) to induce gene expression in the medulla zone of the LG [10], *P{w+mC=r4-GAL4}3*(BDSC, #BL33832) for FB (FB)-specific gene expression [7,13]. All *Drosophila* stocks were maintained on standard cornmeal food at 25°C as previously described [7,46]. For an efficient induction of GAL4-dependent gene expression, individuals carrying the *GAL4 driver* gene and *UAS transgenes* were raised at 28°C. The fly food was prepared according to a previous procedure [46].

4.2. Sample Preparation and Immunostaining of LGs in Larvae

As *mxc^{mbn1}* was maintained in the stock balanced by *FM7a, P{w[+mC]=sChFP}1* carrying the marker gene RFP, mature larvae hemizygous for mxcmbn1 at the third instar stage were selected based on the absence of RFP fluorescence. Normal control males (*w/Y*) pupated at 6 d (28°C) and 7 d (25°C) after egg laying (AEL), whereas the *mxc^{mbn1}* males remained in 3rd instar larval stage at 8 d (28°C) and 10 d (25°C) AEL. A comparison between the control and *mxc^{mbn1}* larvae was performed on the same day that the wandering larvae at the third-instar stage appeared to minimize a delay that might allow hyperplastic tissue to grow. To obtain the larvae, five *pairs of flies were* maintained in culture tubes and allowed to *lay eggs for 24 h* on food. To compare the sizes of the LGs, a pair of anterior lobes of the LG from mature larvae at the third-instar stage was collected and fixed in paraformaldehyde. After staining with DAPI solution (#5748, FUJIFILM Wako Pure Chemical, Osaka, Japan), the fixed LG samples embedded in Vector Shield (#H-1000, Vector Laboratories, Newark, CA, USA) were gently flattened under a covered glass to prepare specimens of a constant thickness [7]. Specimens were observed under a fluorescence microscope (I×81; Olympus Co., Tokyo, Japan) equipped with a CCD camera (ORCA-R2; Hamamatsu Photonics, Hamamatsu, Japan). MetaMorph (version 7.8 13.0, Molecular Devices Inc., San Jose, CA, USA) was used for image processing. The lobe areas of all LGs were measured from the fluorescence images of DAPI-stained samples using ImageJ (version 1.47, National Institutes of Health, Bethesda, MD, USA).

After the fixed LGs were blocked in 10% NGS in PBST (PBS supplemented with 0.1% Triton X-100), the specimens were incubated with anti-Eiger antibody ([25], a gift from M. Miura, Tokyo University) overnight at 4°C. Alexa Fluor 488-conjugated anti-rabbit and anti-mouse IgG antibodies (#A11008 and #A1100, Thermo Fisher Scientific, Oregon, USA) were used to detect the primary antibody. Fluorescence images of the immunostained samples were acquired as described above.

4.3. Preparation of Hemocytes in Drosophila Larval Hemolymph and Immunostaining of the Hemocytes

Mature third instar larvae were dissected in a Drosophila Ringer solution (3 mM $CaCl_2$-$2H_2O$, 182 mM KCl, 46 mM NaCl, 10 mM Tris-base) containing 0.02 μg/mL 1-phenyl-2-thioureic acid (#166-13702, FUJIFILM Wako Pure Chemical, Osaka, Japan). The cells in the hemolymph were allowed to

 doi:10.20944/preprints202410.0708.v1

adhere to a glass slide and fixed in 4% paraformaldehyde solution. After staining with DAPI, the specimens were observed under a fluorescence microscope controlled by MetaMorph (version 7.8 13.0; Molecular Devices Inc., San Jose, CA, USA), as described above.

Hemocytes collected and fixed as described above were blocked with 10% NGS in PBS and incubated with anti-JNK/SAPK antibody (#559304, Merck, Darmstadt, Germany) to detect phosphorylated JNK expression, anti-β-galactosidase antibody (#02150039, MP Biomedicals, Irvine, CA, USA) to monitor the LacZ reporter expression, or anti-Mmp1 antibody (3A6B4, 3B8D12 and 5H7B11, DSHB, IA, USA) [47]overnight at 4°C. To detect the HA-TotF incorporated in the hemocytes localized on the LGs, anti-HA antibody (#2367, Cell Signaling Technology, Danvers, MA, USA) was used. To detect each primary antibody that reacted with the samples, Alexa Fluor 488- or 594-conjugated anti-rabbit or anti-mouse IgG antibodies (#A11008, Thermo Fisher, Oregon, USA) were used according to the animal species in which the primary antibodies were created. Fluorescence images of the samples were acquired as previously described.

To detect the HA-TotF protein incorporated in the hemocytes closely associated with the LGs, the tissues were collected and rinsed with PBS several times before fixation. The LGs, together with associated hemocytes, were fixed with 3.7% paraformaldehyde and blocked with 10% NGS in PBS. Anti-HA immunostaining was performed as described above.

4.4. Transplantation of Hemocytes in Drosophila Larvae

A constant volume of larval hemolymph containing circulating hemocytes was injected into a recipient third-instar larva using glass needles, as previously described [9]. The needles were prepared from G1.2 (Narishige Co., Tokyo, Japan) using a grass puller (PN-31, Narishige Co., Tokyo, Japan) and used after the tip was sharpened. The hemolymph was injected within 5 m of dissection of the recipient larvae to avoid melanization and clogging. After injection, the larvae were placed on wet blocking papers for 1 h to recover from the damage and raised on standard food for 15 h before observation.

4.5. Quantitative Real-Time PCR (qRT-PCR)

Total RNA was extracted from larval FB at the third instar stage using TRIzol reagent (Invitrogen, Waltham, MA, USA). cDNA was synthesized from total RNA using a PrimeScript High Fidelity RT-PCR Kit (TaKaRa, Clontech Laboratories, Shiga, Japan) with oligo dT primers. Real-time PCR was performed using the following qPCR primers: RP49-Fw, 5′-TTCCTGGTGCACAACGTG-3′ and RP49-Rv, 5′-TCTCCTTGCGCTTCTTGG-3′; TotF-Fw, 5′- AGGCACGTCAAATGCTCGC-3′ and TotF-Rv, 5′-TGTTGGTTGTTGTGTGCCCG-3′. The PCR reaction was carried out using a cycling program consisting of an initial denaturation at 95℃ for 5 m, followed by 40 cycles at 95℃ for 5 s and 60℃ for 30 s. The temperature was increased from 60℃ to 95℃ at a rate of 0.1℃/s. Real-time PCR was performed on a Thermal Cycler Dice® Real Time System III (TaKaRa bio., Shiga, Japan) using TB Green Premix Ex Taq II (#RR820A, TaKaRa Bio, Shiga, Japan). Each sample was analyzed in triplicate on a PCR plate, and the final results were obtained by averaging three biological replicates. For quantification, the ΔΔCt method was used to determine the differences between target gene expression and that of the reference gene, Rp49.

4.6. Statistical Analysis

Scatter plots were created using GraphPad Prism 9 (GraphPad Software, San Diego, CA, USA) or Microsoft Office Excel 2016 (Microsoft, Redmond, WA, USA) to determine the number of hemocytes in the LGs and FB. The fluorescence intensity of LGs or circulating hemocytes was quantified using ImageJ (Ver.1.54h, National Institutes of Health, Bethesda, MD, USA). Each dataset was assessed using Welch's *t*-test as previously described [8,23,47]. Before then, an F-test was performed to determine equal or unequal variances. Welch's *t*-test was performed when the value was less than 0.05 (unequal variance), whereas Student's *t*-test was performed when the value was

greater than 0.05 (with equal variance). One-way analysis of variance (ANOVA) was used to analyze differences among groups. A *p*-value of 0.05 or less was considered statistically significant.

Supplementary Materials: The following supporting information can be downloaded at the website of this paper posted on Preprints.org, Figure S1: Enhancement of the LG tumor's growth in the *mxc*^{mbn1} larvae harboring the *Upd3*-depleted circulating hemocytes; Figure S2: Anti-MMP1 immunostaining of the normal circulating hemocytes transplanted into control and *mxc*^{mbn1} larvae; Figure S3: Enhancement of the LG tumor's growth in *mxc*^{mbn1} larvae harboring *wgn*- or *grnd*- depleted circulating hemocytes.

Author Contributions: Formal analysis and investigation: J.K. and Y.K.; Writing the original draft :J.K. and Y.H.I. Y.K. contributed to the initial stages of the study and writing a part of the original draft. Supervision, Y.H.I.; project administration, Y.H.I.; funding acquisition, Y.H.I.; writing—review and editing, Y.H.I.; visualization, Y.H.I.; supervision, Y.H.I. and T.N. All authors have read and agreed to the published version of the manuscript.

Funding: This study was partially funded by a JSPS KAKENHI Grant-in-Aid for Scientific Research C, grant number 17K07500, awarded to Y.H.I.

Institutional Review Board Statement: The animal study protocol was approved by the Kyoto Institute of Technology Review Board (protocol code: R4-11 and date of approval: January 24 2023).

Informed Consent Statement: Not applicable.

Data Availability Statement: The datasets generated and/or analyzed in the current study are available from the corresponding author on reasonable request.

Acknowledgments: J.K. was supported by a scholarship from the Japan Student Services Organization (JASSO). We thank A. Watanabe and Mina Plat for their technical assistance. We acknowledge M. Miura (Tokyo university) and DSHB (Iowa university) for providing antibodies, and N. Perrimon (Harvard university), Bloomington Stock Center, Fly ORF Center, and Vienna Drosophila Stock Center for providing fly stocks.

Conflicts of Interest: The authors declare no conflicts of interest.

References

1. Huang, Y.; Pang, Y.; Xu, Y.; Liu, L.; Zhou, H. The identification of regulatory ceRNA network involved in *Drosophila* Toll immune responses. *Dev. Comp. Immunol.* **2024**, *151*, 105105, doi:10.1016/j.dci.2023.105105.
2. Lemaitre, B.; Hoffmann, J. The host defense of Drosophila melanogaster. *Annu. Rev. Immunol.* **2007**, *25*, 697–743, doi:10.1146/annurev.immunol.25.022106.141615.
3. Ekengren, S.; Hultmark, D. A family of *Turandot*-related genes in the humoral stress response of *Drosophila*. *Biochem. Biophys. Res. Commun.* **2001**, *284*, 998–1003, doi:10.1006/bbrc.2001.5067.
4. Bland, M.L. Regulating metabolism to shape immune function: Lessons from *Drosophila*. *Semin. Cell Dev. Biol.* **2023**, *138*, 128–141, doi:10.1016/j.semcdb.2022.04.002.
5. Valanne, S.; Wang, J.-H.; Rämet, M. The Drosophila Toll signaling pathway. *J. Immunol.* **2011**, *186*, 649–656, doi:10.4049/jimmunol.1002302.
6. Myllymäki, H.; Valanne, S.; Rämet, M. The Drosophila Imd signaling pathway. *J. Immunol.* **2014**, *192*, 3455–3462, doi:10.4049/jimmunol.1303309.
7. Araki, M.; Kurihara, M.; Kinoshita, S.; Awane, R.; Sato, T.; Ohkawa, Y.; Inoue, Y.H. Anti-Tumour effects of antimicrobial peptides, components of the innate immune system, against haematopoietic tumours in *Drosophila mxc* mutants. *Dis. model. mech.* **2019**, *12*, dmm037721, doi:10.1242/dmm.037721.
8. Parvy, J.-P.; Yu, Y.; Dostalova, A.; Kondo, S.; Kurjan, A.; Bulet, P.; Lemaître, B.; Vidal, M.; Cordero, J.B. The antimicrobial peptide defensin cooperates with tumour necrosis factor to drive tumour cell death in *Drosophila*. *eLife* **2019**, *8*, e45061, doi:10.7554/eLife.45061.
9. Kinoshita, S.; Takarada, K.; Kinoshita, Y.; Inoue, Y.H. *Drosophila* hemocytes recognize lymph gland tumors of *mxc* mutants and activate the innate immune pathway in a reactive oxygen species-dependent manner. *Biol. Open* **2022**, *11*, bio059523, doi:10.1242/bio.059523.
10. Agaisse, H.; Petersen, U.-M.; Boutros, M.; Mathey-Prevot, B.; Perrimon, N. Signaling role of hemocytes in *Drosophila* JAK/STAT-dependent response to septic injury. *Dev. Cell* **2003**, *5*, 441–450, doi:10.1016/S1534-5807(03)00244-2.
11. Romão, D.; Muzzopappa, M.; Barrio, L.; Milán, M. The Upd3 cytokine couples inflammation to maturation defects in *Drosophila*. *Curr. Biol.* **2021**, *31*, 1780-1787.e6, doi:10.1016/j.cub.2021.01.080.
12. Myllymäki, H.; Rämet, M. JAK/STAT pathway in *Drosophila* immunity. *Scand. J. Immunol.* **2014**, *79*, 377–385, doi:10.1111/sji.12170.
13. Kinoshita, Y.; Shiratsuchi, N.; Araki, M.; Inoue, Y.H. Anti-tumor effect of Turandot proteins induced via the JAK/STAT pathway in the *mxc* hematopoietic tumor mutant in *Drosophila*. *Cells* **2023**, *12*, 2047, doi:10.3390/cells12162047.

14. Moreno, E.; Basler, K.; Morata, G. Cells compete for Decapentaplegic survival factor to prevent apoptosis in *Drosophila* wing development. *Nature* **2002**, *416*, 755–759, doi:10.1038/416755a.
15. Igaki, T. Correcting developmental errors by apoptosis: lessons from *Drosophila* JNK signaling. *Apoptosis* **2009**, *14*, 1021–1028, doi:10.1007/s10495-009-0361-7.
16. La Marca, J.E.; Richardson, H.E. Two-faced: roles of JNK signalling during tumourigenesis in the *Drosophila* model. *Front. Cell Dev. Biol.* **2020**, *8*, doi:10.3389/fcell.2020.00042.
17. Gold, K.S.; Brückner, K. Macrophages and cellular immunity in *Drosophila melanogaster*. *Semin. Immunol.* **2015**, *27*, 357–368, doi:10.1016/j.smim.2016.03.010.
18. Meister, M.; Lagueux, M. Drosophila blood cells. *Cell. Microbiol.* **2003**, *5*, 573–580, doi:10.1046/j.1462-5822.2003.00302.x.
19. Williams, M.J. Drosophila hemopoiesis and cellular immunity. *J. Immuno.* **2007**, *178*, 4711–4716, doi:10.4049/jimmunol.178.8.4711.
20. Jung, S.-H.; Evans, C.J.; Uemura, C.; Banerjee, U. The *Drosophila* lymph gland as a developmental model of hematopoiesis. *Development* **2005**, *132*, 2521–2533, doi:10.1242/dev.01837. 1.
21. Shrestha, R.; Gateff, E. Ultrastructure and cytochemistry of the cell types in the larval hematopoietic organs and hemolymph of *Drosophila melanogaster*. *Dev. Growth Differ.* **1982**, *24*, 65–82, doi:10.1111/j.1440-169X.1982.00065.x.
22. Remillieux-Leschelle, N.; Santamaria, P.; Randsholt, N.B. Regulation of larval hematopoiesis in *Drosophila melanogaster*: A role for the *multi sex combs* gene. *Genetics* **2002**, *162*, 1259–1274, doi:10.1093/genetics/162.3.1259.
23. Kurihara, M.; Komatsu, K.; Awane, R.; Inoue, Y.H. Loss of histone locus bodies in the mature hemocytes of larval lymph gland result in hyperplasia of the tissue in *mxc* mutants of *Drosophila*. *Int. J. Mol. Sci.* **2020**, *21*, 1586, doi:10.3390/ijms21051586.
24. Takarada, K.; Kinoshita, J.; Inoue, Y.H. Ectopic expression of matrix metalloproteinases and filopodia extension via JNK activation are involved in the invasion of blood tumor cells in *Drosophila mxc* mutant. *Genes Cells* **2023**, *28*, 709–726, doi:10.1111/gtc.13060.
25. Igaki, T.; Pastor-Pareja, J.C.; Aonuma, H.; Miura, M.; Xu, T. Intrinsic tumor suppression and epithelial maintenance by endocytic activation of Eiger/TNF signaling in *Drosophila*. *Dev. Cell* **2009**, *16*, 458–465, doi:10.1016/j.devcel.2009.01.002.
26. Herrera, S.C.; Bach, E.A. The emerging roles of JNK signaling in Drosophila stem cell homeostasis. *Int. J. Mol. Sci.* **2021**, *22*, 5519, doi:10.3390/ijms22115519.
27. Oldefest, M.; Nowinski, J.; Hung, C.-W.; Neelsen, D.; Trad, A.; Tholey, A.; Grötzinger, J.; Lorenzen, I. Upd3 – An ancestor of the four-helix bundle cytokines. *Biochem. Biophys. Res. Commun.* **2013**, *436*, 66–72, doi:10.1016/j.bbrc.2013.04.107.
28. Narasimamurthy, R.; Geuking, P.; Ingold, K.; Willen, L.; Schneider, P.; Basler, K. Structure-function analysis of Eiger, the *Drosophila* TNF homolog. *Cell Res.* **2009**, *19*, 392–394, doi:10.1038/cr.2009.16.
29. Bunker, B.D.; Nellimoottil, T.T.; Boileau, R.M.; Classen, A.K.; Bilder, D. The transcriptional response to tumorigenic polarity loss in *Drosophila*. *eLife* **2015**, *4*, e03189, doi:10.7554/eLife.03189.
30. Hultmark, D.; Ekengren, S. A cytokine in the *Drosophila* stress response. *Dev. Cell* **2003**, *5*, 360–361, doi:10.1016/S1534-5807(03)00268-5.
31. Knüpfer, H.; Preiß, R. Significance of interleukin-6 (IL-6) in breast cancer (review). *Breast Cancer Res. Treat.* **2007**, *102*, 129–135, doi:10.1007/s10549-006-9328-3.
32. Pastor-Pareja, J.C.; Wu, M.; Xu, T. An innate immune response of blood cells to tumors and tissue damage in *Drosophila*. *Dis. model. mech.* **2008**, *1*, 144–154, doi:10.1242/dmm.000950.
33. Kochumon, S.; Al-Sayyar, A.; Jacob, T.; Hasan, A.; Al-Mulla, F.; Sindhu, S.; Ahmad, R. TNF-α increases IP-10 expression in MCF-7 breast cancer cells via activation of the JNK/c-Jun pathways. *Biomolecules* **2021**, *11*, 1355, doi:10.3390/biom11091355.
34. Moreno, E.; Yan, M.; Basler, K. Evolution of TNF signaling mechanisms: JNK-dependent apoptosis triggered by Eiger, the *Drosophila* homolog of the TNF superfamily. *Curr. Biol.* **2002**, *12*, 1263–1268, doi:10.1016/S0960-9822(02)00954-5.
35. Pan, Y.; Yu, Y.; Wang, X.; Zhang, T. Tumor-associated macrophages in tumor immunity. *Front. Immunol.* **2020**, *11*, doi:10.3389/fimmu.2020.583084.
36. Chen, J.; Yao, Y.; Gong, C.; Yu, F.; Su, S.; Chen, J.; Liu, B.; Deng, H.; Wang, F.; Lin, L.; et al. CCL18 from tumor-associated macrophages promotes breast cancer metastasis via PITPNM3. *Cancer Cell* **2011**, *19*, 814–816, doi:10.1016/j.ccr.2011.05.024.
37. Jinushi, M.; Chiba, S.; Yoshiyama, H.; Masutomi, K.; Kinoshita, I.; Dosaka-Akita, H.; Yagita, H.; Takaoka, A.; Tahara, H. Tumor-associated macrophages regulate tumorigenicity and anticancer drug responses of cancer stem/Initiating cells. *Proc. Natl. Acad. Sci. U.S. A.* **2011**, *108*, 12425–12430, doi:10.1073/pnas.1106645108.
38. Aiello, A.; Giannessi, F.; Percario, Z.A.; Affabris, E. An emerging interplay between extracellular vesicles and cytokines. *Cytokine Growth Factor Rev.* **2020**, *51*, 49–60, doi:10.1016/j.cytogfr.2019.12.003.

39. Ruan, W.; Srinivasan, A.; Lin, S.; Kara, k-I.; Barker, P.A. Eiger-induced cell death relies on Rac1-dependent endocytosis. *Cell Death Dis.* **2016**, *7*, e2181–e2181, doi:10.1038/cddis.2016.80.
40. Chang, H.F.; Schirra, C.; Ninov, M.; Hahn, U.; Ravichandran, K.; Krause, E.; Becherer, U.; Bálint, Š.; Harkiolaki, M.; Urlaub, H.; Valitutti, S.; Baldari, C.T.; Dustin, M.L.; Jahn, R.; Rettig, J. Identification of distinct cytotoxic granules as the origin of supramolecular attack particles in T lymphocytes. *Nat. Commun.* **2022**, *13*, 1029. doi:10.1038/s41467-022-28596-y
41. Woodcock, K.J.; Kierdorf, K.; Pouchelon, C.A.; Vivancos, V.; Dionne, M.S.; Geissmann, F. Macrophage-derived upd3 cytokine causes impaired glucose homeostasis and reduced lifespan in *Drosophila* fed a lipid-rich diet. *Immunity* **2015**, *42*, 133-144., doi: 10.1016/j.immuni.2014.12.023
42. Hodgson, J.A.; Parvy, J.P.; Yu, Y.; Vidal, M.; Cordero, J.B. *Drosophila* larval models of invasive tumorigenesis for in vivo studies on Tumour/Peripheral host tissue interactions during cancer cachexia. *Int. J. Mol. Sci.* **2021**, *22*, 8317. doi: 10.3390/ijms22158317
43. Andersen, D.S.; Colombani, J.; Palmerini, V.; Chakrabandhu, K.; Boone, E.; Röthlisberger, M.; Toggweiler, J.; Basler, K.; Mapelli, M.; Hueber, A.O.; Léopold, P. The *Drosophila* TNF receptor Grindelwald couples loss of cell polarity and neoplastic growth. *Nature* **2015**, *522*, 482-486. doi: 10.1038/nature14298
44. Sopko, R.; Foos, M.; Vinayagam, A.; Zhai, B.; Binari, R.; Hu, Y.; Randklev, S.; Perkins, L.A.; Gygi, S.P.; Perrimon, N. Combining genetic perturbations and proteomics to examine kinase-phosphatase networks in Drosophila embryos. *Dev. Cell* **2014**, *31*, 114-127. doi:10.1016/j.devcel.2014.07.027
45. Stofanko, M.; Kwon, S.Y.; Badenhorst, P. A Misexpression screen to identify regulators of Drosophila larval hemocyte development. *Genetics* **2008**, *180*, 253–267, doi:10.1534/genetics.108.089094.
46. Oka, S.; Hirai, J.; Yasukawa, T.; Nakahara, Y.; Inoue, Y.H. A correlation of reactive oxygen species accumulation by depletion of superoxide dismutases with age-dependent impairment in the nervous system and muscles of Drosophila adults. *Biogerontol.* **2015**, *16*, 485–501, doi:10.1007/s10522-015-9570-3.
47. Kurihara, M.; Takarada, K.; Inoue, Y.H. Enhancement of leukemia-like phenotypes in *Drosophila mxc* mutant larvae due to activation of the RAS-MAP kinase cascade possibly via down-regulation of DE-Cadherin. *Genes Cells* **2020**, *25*, 757–769, doi:10.1111/gtc.12811.